



OPEN

Novel magnetic propylsulfonic acid-anchored isocyanurate-based periodic mesoporous organosilica (Iron oxide@PMO-ICS-PrSO₃H) as a highly efficient and reusable nanoreactor for the sustainable synthesis of imidazopyrimidine derivatives

Arezoo Akbari, Mohammad G. Dekamin[✉], Amene Yaghoubi & Mohammad Reza Naimi-Jamal

In this study, preparation and characterization of a new magnetic propylsulfonic acid-anchored isocyanurate bridging periodic mesoporous organosilica (Iron oxide@PMO-ICS-PrSO₃H) is described. The iron oxide@PMO-ICS-PrSO₃H nanomaterials were characterized by Fourier transform infrared spectroscopy, energy-dispersive X-ray spectroscopy and field emission scanning electron microscopy as well as thermogravimetric analysis, N₂ adsorption–desorption isotherms and vibrating sample magnetometer techniques. Indeed, the new obtained materials are the first example of the magnetic thermally stable isocyanurate-based mesoporous organosilica solid acid. Furthermore, the catalytic activity of the Iron oxide@PMO-ICS-PrSO₃H nanomaterials, as a novel and highly efficient recoverable nanoreactor, was investigated for the sustainable heteroannulation synthesis of imidazopyrimidine derivatives through the Traube–Schwarz multicomponent reaction of 2-aminobenzoimidazole, C–H acids and diverse aromatic aldehydes. The advantages of this green protocol are low catalyst loading, high to quantitative yields, short reaction times and the catalyst recyclability for at least four consecutive runs.

The use of heterogeneous catalysts has been developed because of their desirable properties and addressing many principles of green chemistry. Therefore, development and research in the heterogeneous catalysts has received major consideration due to disadvantages associated with homogeneous catalysts such as catalyst recovery, product separation, corrosion problems and environmental hazards^{1–5}. Along these lines, development of nanoporous materials with significant improved properties is a new and growing research field in the recent years^{6–10}. Highly-ordered periodic mesoporous organosilicas (PMOs) materials, as a kind of inorganic-organic hybrid mesoporous materials, have attracted significant interest because of their noteworthy properties such as high surface area, narrow pore size distribution, adjustable mesopore diameter, high mechanical and hydrothermal stability, and highly tunable physicochemical properties by varying the nature and extent of the surface functionalization.

PMOs which are mainly prepared from bridged organosilane precursors [(R'O)₃Si-R-Si(OR')₃; R: organic bridging group, R': methyl or ethyl] have found vast applications in various fields such as drug delivery systems, absorption and storage of mechanical energy, gas storage, electronics, sensors, luminescence, adsorbents,

Pharmaceutical and Heterocyclic Compounds Research Laboratory, Department of Chemistry, Iran University of Science and Technology, Tehran 1684613114, Iran. ✉email: mdekamin@iust.ac.ir

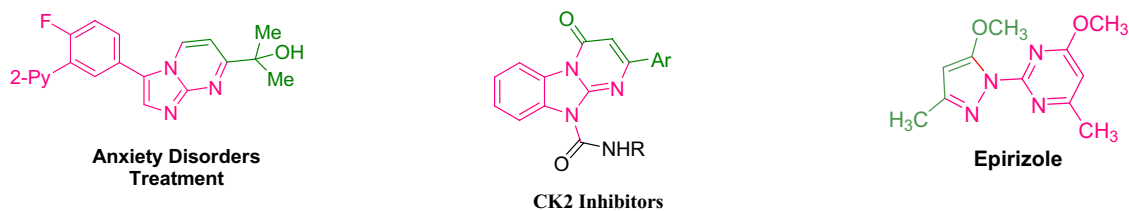


Figure 1. Representative examples of biologically active imidazopyrimidine derivatives.

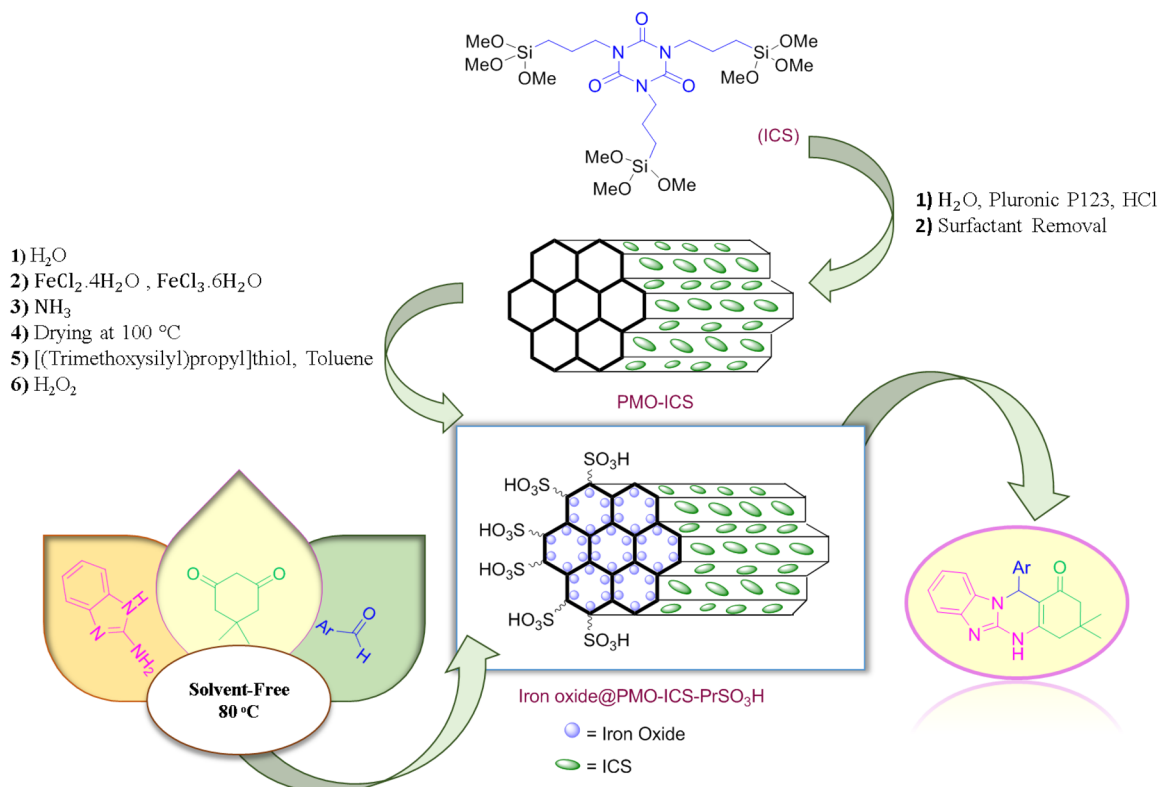
chromatography, solid-phase extraction, etc. Also, these type of materials have been used as suitable supports in a diversity of heterogeneous catalysts for different organic reactions^{11–29}. Indeed, the mesopore channels and high surface area of PMOs make them as an appropriate nanoreactor for releasing of the reactants into mesoporous channels and increases the reaction rate^{30–41}. In addition to the above mentioned properties, another special features of PMOs are uniform distribution of active organic groups within their framework to tune their polarity compared to nanoordered silica materials and reusability¹³. Among the various organic groups used in the PMOs structure, the heteroaromatic isocyanurate ring containing three nonpolar alkyl groups shows excellent properties including nontoxicity, highly branched, binding ability to transition metals and high thermal stability^{14,34,35,42–47}. On the other hand, the inclusion of magnetic nanoparticles (MNPs) in the modified materials allows convenient and cost-effective separation to be conveniently performed by an external magnetic field instead of centrifugation and filtration steps. Furthermore, MNPs enhance the reaction rates by local heating through induction as well as providing appropriate surface area. Also, they show synergistic effects in combination to other catalytic species or centers, due to the catalytic performance of magnetic materials, including Fe, Ni, or Co-based ones^{27,48–54}. Therefore, the synergistic effects of both PMO-based organosilicas and magnetic components for designing and application of new materials would be very desirable. To the best of our knowledge, a little efforts have been made for designing of magnetic PMO materials^{54–56}, especially thermally stable isocyanurate-based mesoporous organosilica solid acid which are in high demand for promoting of organic reactions at elevated temperatures.

On the other hand, development of simple synthetic procedures for the synthesis of complex and diversity-oriented organic molecules from readily available substrates is an important challenge in organic and medicinal chemistry. This can be achieved through multicomponent reactions (MCRs) strategy as a powerful process for the synthesis of molecules useful for pharmaceuticals, biological studies, secret communication and electronic including heterocyclic scaffolds^{57–62} as well as fabrication of new task-specific materials such as drug delivery systems, nanocomposites, polymers, supramolecular systems and molecular machines^{63–68}. In MCRs, three or more reactants simultaneously combine together in one reaction vessel to form a final product with high bond forming index such as imidazopyrimidine derivatives^{69–77}. Indeed, imidazopyrimidine derivatives show a diverse range of biological and pharmacological activities such as CK2 inhibitor as well as for the treatment of anxiety disorders and ulcers, etc. (Fig. 1)^{78–82}.

Because of the importance of imidazopyrimidine scaffold, different homogeneous or heterogeneous acidic catalytic systems have been investigated to promote multicomponent condensation of 2-aminobenzimidazole, aromatic aldehydes and C–H acids such as dimedone/malononitrile or relevant synthons. Some of the recent examples of reported catalysts are $H_6P_2W_{18}O_{62} \cdot 18H_2O$ ⁸³, WO_3 -supported sulfonic acid⁸⁴, O-sulfonated poly(vinylpyrrolidonium) hydrogen sulfate⁸⁵, modified ZnO nanoparticles under ball milling conditions⁸⁶, organo-sulfonic acid tags anchored on magnetic titania coated $NiFe_2O_4$ nanoparticles⁸⁷, $Fe_3O_4@GO$ ⁸⁸, magnetic Irish moss⁸⁰, carboxymethyl cellulose⁸⁹, NH_2SO_3H ⁹⁰, *p*-toluenesulfonic acid monohydrate^{91,92}, $Fe_3O_4@clay$ ⁹³, L-proline⁹⁴, molecular iodine⁹⁵, polyethylene glycol methacrylate-grafted dicationic imidazolium-based ionic liquid⁹⁶ and $NaHSO_4$ modified phenylene bridged periodic mesoporous organosilica magnetic nanoparticles⁹⁵. In spite of their merits, the existing methodologies have drawbacks such as low to moderate yields, difficulties in the catalyst recovery and product isolation, toxic or expensive catalysts, lengthy reaction times, the use of volatile organic solvents or significant amounts of waste materials production⁹⁷. Therefore, development of new methodologies and introducing green catalysts to overcome the aforementioned drawbacks is still favorable. To address limitations and disadvantages associated with these catalytic systems, preparation and catalytic application of magnetic isocyanurate-based propylsulfonic acid periodic mesoporous organosilica (Iron oxide@PMO-ICS- $PrSO_3H$), as a novel and highly efficient heterogeneous mesoporous catalyst, would be very desirable. In continuation of our research interest to develop and improve novel and efficient catalysts for different MCRs or organic transformations^{34,35,51,52,73,74,89,98,99}, we wish herein to report the application of Iron oxide@PMO-ICS- $PrSO_3H$ (**1**), as a novel recyclable catalyst, for the synthesis of imidazopyrimidine derivatives through the Traube–Schwarz multicomponent reaction under solvent-free conditions. To the best of our knowledge, there is no report on the use of Iron oxide@PMO-ICS- $PrSO_3H$, as a nano-architected heterogeneous and recoverable catalyst, for different organic transformations (Scheme 1).

Results and discussion

Characterization of the Iron oxide@PMO-ICS- $PrSO_3H$ nanomaterials (1**).** After preparation of the magnetic isocyanurate-based propylsulfonic acid periodic mesoporous organosilica (Iron oxide@PMO-ICS- $PrSO_3H$) nanocatalyst (**1**), its composition, structure, morphology and textural properties was properly characterized by different methods and techniques. The FT-IR spectra of both magnetic Iron oxide@PMO-ICS (**B**) and Iron oxide@PMO-ICS- $PrSO_3H$ (**1**) nanomaterials have been compared in Fig. 2. As it can be seen in Fig. 2, the



Scheme 1. Schematic preparation of the Iron oxide@PMO-ICS-PrSO₃H nanocatalyst (1) and its application in the synthesis of imidazopyrimidine derivatives **6a–g** and **7a–g**.

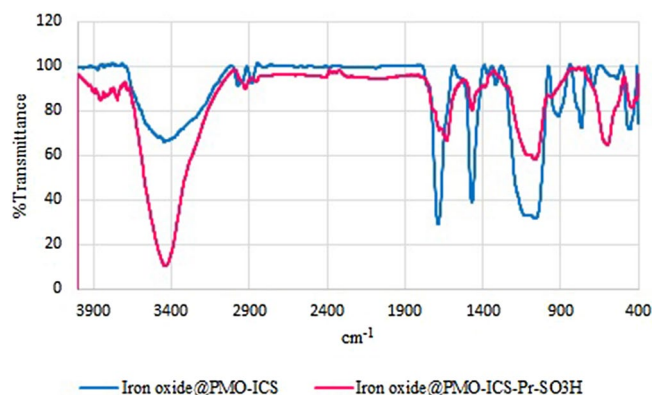


Figure 2. FT-IR spectra of PMO-ICS mesoporous catalyst (blue spectrum) and Iron oxide@PMO-ICS-PrSO₃H magnetic mesoporous catalyst (1, pink spectrum).

absorbance bands at $2,925$ and $2,857\text{ cm}^{-1}$ are related to C–H stretching of the aliphatic moiety in the catalyst **1** or its precursor nanomaterials B. Furthermore, absorption bands in the regions $1,120$, $1,070$ and 933 cm^{-1} correspond to the asymmetric and symmetric vibrations of Si–O–Si (siloxane) vibrations, respectively. Moreover, the signals appeared at $1,633$ and $1,470\text{ cm}^{-1}$ are attributed to the stretching vibrations of the isocyanurate ring. Also, the absorption bands at $1,284$ – $1,177$ and $1,134$ – $1,045$ as well as 630 – 572 cm^{-1} were assigned to the O=S=O asymmetric or symmetric and S–O stretching vibration of the –SO₃H functional group, respectively. Furthermore, the band observed at 480 cm^{-1} could be attributed to the Fe–O spinel structure.

On the other hand, thermogravimetric analysis (TGA) of the Iron oxide@PMO-ICS-PrSO₃H magnetic catalyst (**1**) demonstrated three weight losses at different temperature ranges. The first one, with 4.96% weight loss between 25 and $100\text{ }^\circ\text{C}$, is corresponded to the removing of water and alcoholic solvents remaining from the extraction process. The second and very small weight loss (1.82%) at 100 to $260\text{ }^\circ\text{C}$ region is attributed to the elimination of surfactant template of the synthesis process. Finally, the main weight loss (20.10%) which observed

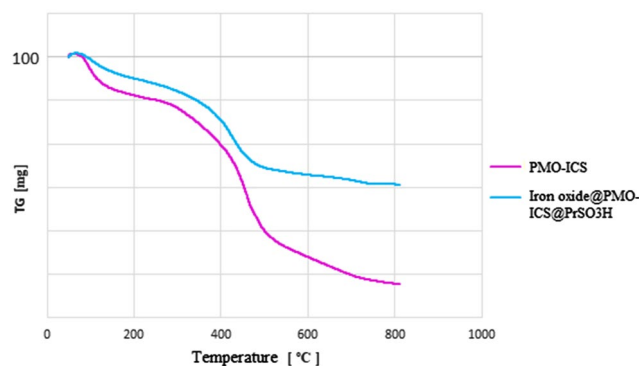


Figure 3. TGA analysis of pure PMO-ICS (purple curve) and Iron oxide@PMO-ICS-PrSO₃H mesoporous catalysts (**1**, blue curve).

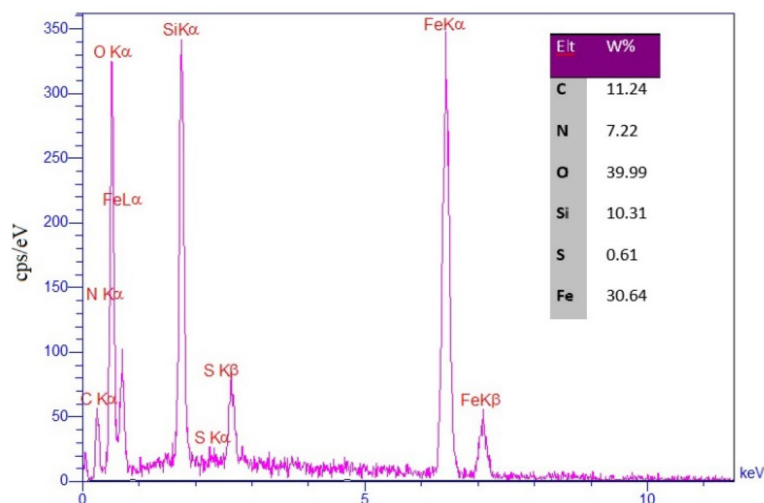


Figure 4. The EDX spectrum of the Iron oxide@PMO-ICS-PrSO₃H mesoporous catalyst (**1**).

in the range of 260–800 °C, is attributed to the removing of organic functional groups including propylenesulfonic acid and 1,3,5-tris(1,3-propylen) isocyanurate moiety incorporated in the material framework (Fig. 3).

Furthermore, the composition of Iron oxide@PMO-ICS-PrSO₃H mesoporous catalyst (**1**) was characterized by energy-dispersive X-ray (EDX) spectroscopy. As shown in Fig. 4, signals of C, O, N, Fe, Si and S elements (ratios of 11.24: 39.99: 30.64: 7.22: 10.31: 3.64 wt%, respectively) confirm the successful incorporation of expected elements into the structure of Iron oxide@PMO-ICS-PrSO₃H mesoporous catalyst.

On the other hand, Fig. 5 shows the N₂ adsorption–desorption isotherms and pore size distributions (Barrett–Joyner–Halenda, BJH) of the Iron oxide@PMO-ICS-PrSO₃H mesoporous materials (**1**). The Iron oxide@PMO-ICS-PrSO₃H itself displays a type IV isotherm, with an H₃ hysteresis loop. This analysis demonstrated that the BET specific surface area of the mesoporous materials **1** is close to 175.05 m²/g and it exhibits BJH average pore diameter and total pore volume equal to 7.41 nm and 0.32 cm³/g, respectively.

Moreover, the total acidity of Iron oxide@PMO-ICS-PrSO₃H solid acid (**1**) was calculated through pH analysis of a precisely weighed sample of the material after ion exchange with saturated solution of NaCl. The results demonstrated that the loading of H⁺ on the solid surface is 2.0 mmol.g⁻¹. On the other hand, low-angle XRD patterns of Iron oxide@PMO-ICS-PrSO₃H solid acid (**1**) shows one sharp peak at 2θ = ~0.95 which confirms the presence and preservation of mesoporous framework of the PMO-ICS organosilica as well as its periodicity (Fig. 6).

Furthermore, the morphology of the catalyst (**1**) was characterized by field emission scanning electron microscopy (FESEM). The FESEM images of Iron oxide@PMO-ICS-PrSO₃H powder (**1**) illustrated well-ordered structure of PMO-ICS and almost uniform distribution of propylenesulfonic acid functional group and iron oxide particles with average particle sizes of about 14–32 nm (Fig. 7).

Furthermore, TEM images illustrated the structural order and the morphology of Iron oxide@PMO-ICS-PrSO₃H nanocatalyst (**1**) as well as presence of well distributed iron oxide nanoparticles confined inside of its mesoporous channels (Fig. 8).

Also, the saturation magnetic properties of Iron oxide@PMO-ICS-PrSO₃H mesoporous materials (**1**) were evaluated using VSM technique at room temperature. According to the obtained results shown in Fig. 9, the saturation magnetization of the Iron oxide@PMO-ICS-PrSO₃H mesoporous materials was determined to be

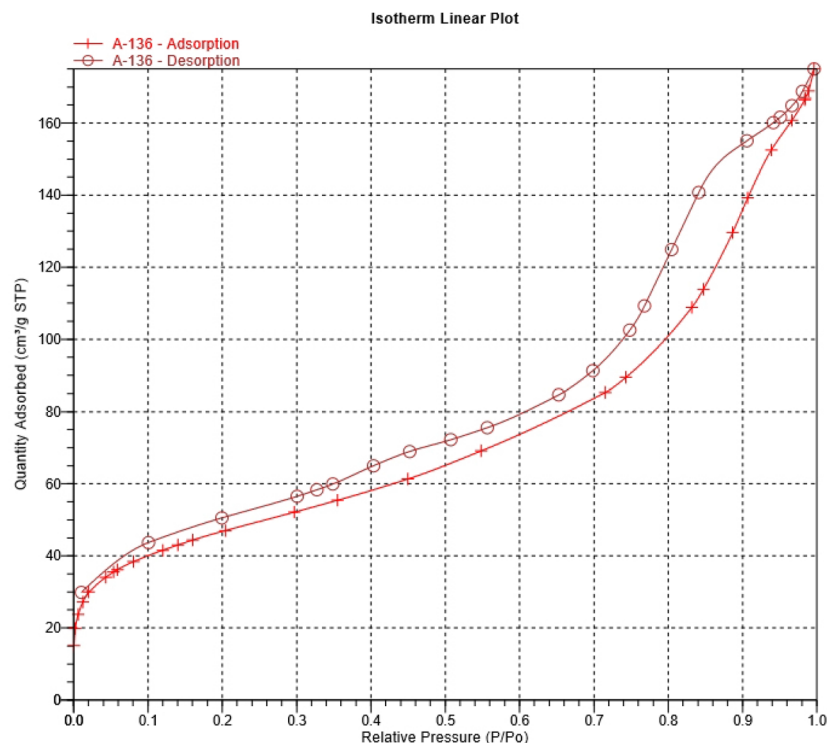


Figure 5. N₂ adsorption–desorption isotherms of the Iron oxide@PMO-ICS-PrSO₃H mesoporous materials (1).

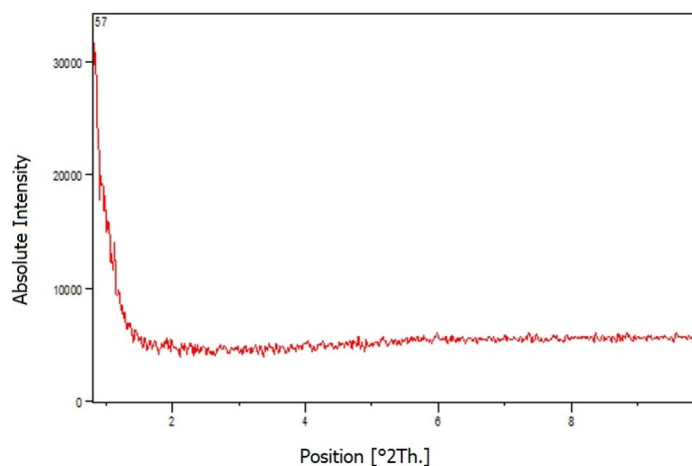


Figure 6. Low-angle XRD patterns of Iron oxide@PMO-ICS-PrSO₃H solid acid (1).

35 emu/g which is lower than that of the parent superparamagnetic iron oxide (55 emu/g) but is sufficiently high for practical applications^{100,101}.

Investigation of the catalytic activity of the Iron oxide@PMO-PrSO₃H nanocatalyst (1) for the synthesis of imidazopyrimidine derivatives 6a–g or 7a–g. In this step, the catalytic activity of the Iron oxide@PMO-PrSO₃H nanocatalyst (1) was investigated for the synthesis of imidazopyrimidine derivatives. Therefore, the reaction of 2-aminobenzimidazole (2) and 4-chlorobenzaldehyde (3a) with dimedone (4) was selected as the model reaction. The obtained results from optimization experiments illustrated that both the catalyst loading and temperature strongly affect the reaction progress which have been summarized in Table 1. Indeed, only a trace amount of the desired product, 12-(4-chlorophenyl)-3,3-dimethyl-3,4,5,12-tetrahydrobenzo[4,5]imidazo[2,1-*b*]quinazolin-1(2*H*)-one (6a), was obtained in the absence of Iron oxide@PMO-ICS-PrSO₃H nanocatalyst (1) after 2 h at 80 °C under solvent-free conditions (Table 1, entry 1). To our

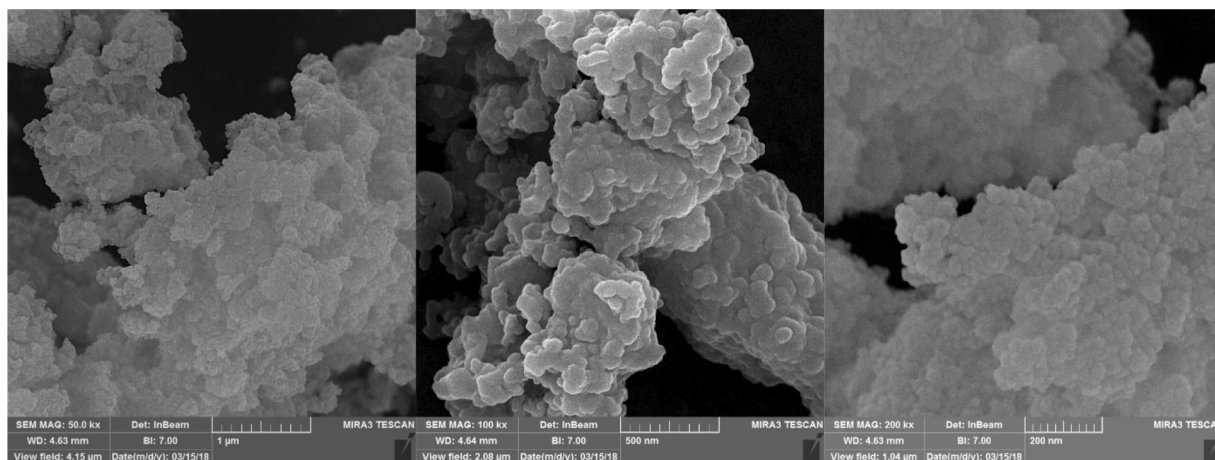


Figure 7. FESEM images of the Iron oxide@PMO-ICS-PrSO₃H magnetic mesoporous nanocatalyst (1).

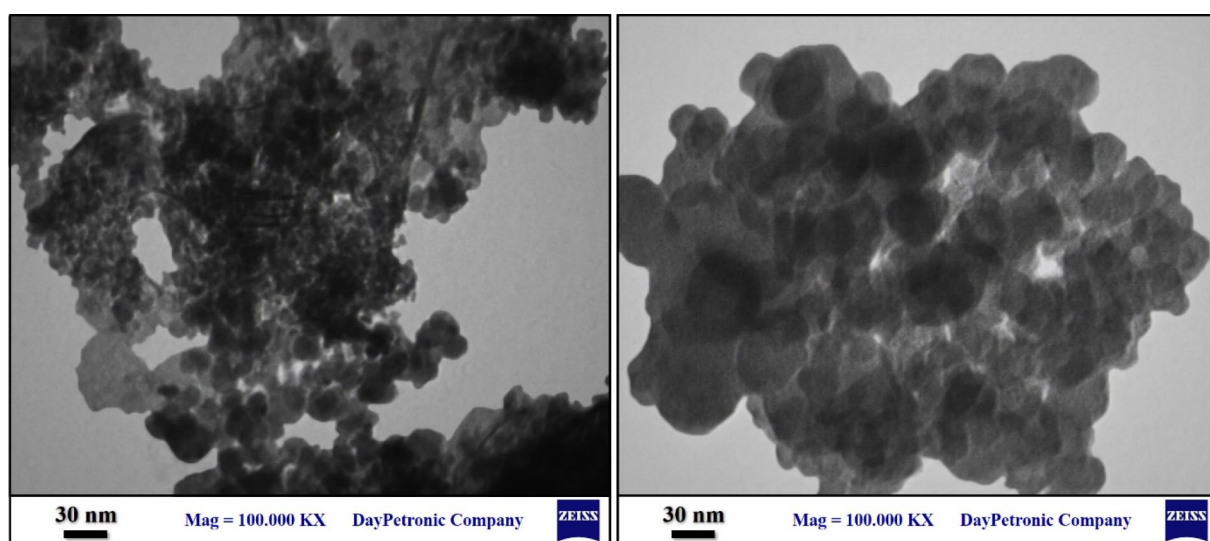


Figure 8. TEM images of Iron oxide@PMO-ICS-PrSO₃H nanocatalyst (1).

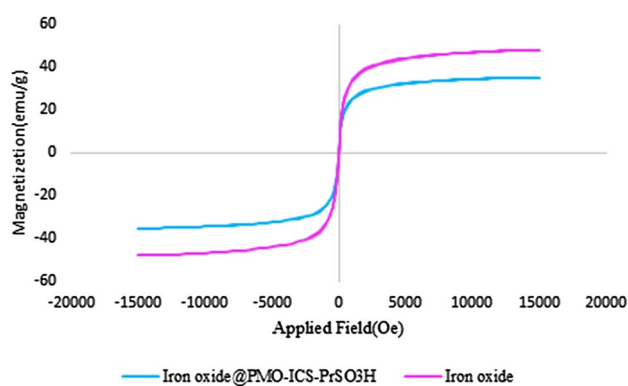
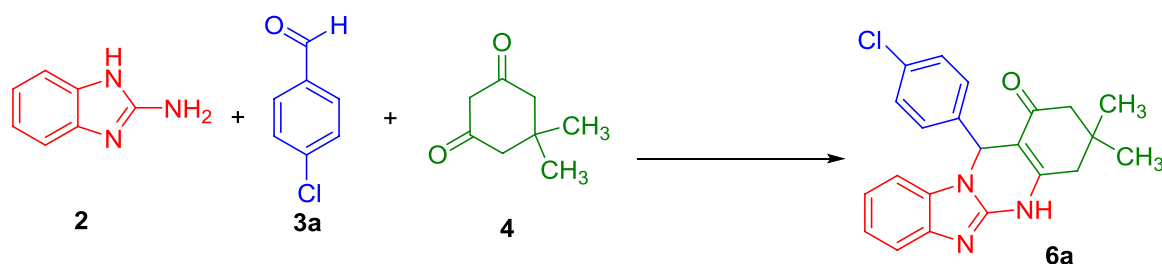


Figure 9. VSM pattern of the iron oxide (purple curve) and the Iron oxide@PMO-ICS-PrSO₃H mesoporous catalyst (1, blue curve).

Entry	Catalyst	Catalyst loading (mg)	Solvent	Temp. (°C)	Time (min)	Yield ^a (%)
1	-	-	Solvent-Free	80	120	Trace
2	Iron oxide@PMO-PrSO ₃ H	7	Solvent-Free	80	15	92
3	Iron oxide@PMO-PrSO ₃ H	10	Solvent-Free	80	10	95
4	Iron oxide@PMO-PrSO ₃ H	15	Solvent-Free	80	10	96
5	Iron oxide@PMO-PrSO ₃ H	20	Solvent-Free	80	7	97
6	Iron oxide@PMO-PrSO ₃ H	10	Solvent-Free	70	15	93
7	Iron oxide@PMO-PrSO ₃ H	10	Solvent-Free	60	20	93
8	Iron oxide@PMO-PrSO ₃ H	10	EtOH/H ₂ O	60	25	82
9	Iron oxide@PMO-PrSO ₃ H	10	THF	Reflux	30	75
10	Iron oxide@PMO	10	Solvent-Free	80	35	65
11	Iron oxide@PMO-PrSH	10	Solvent-Free	80	40	36
12	Iron oxide	10	Solvent-Free	80	70	28
13	PMO-ICS	10	Solvent-Free	80	50	46

Table 1. Optimization of the conditions for the model reaction in the synthesis of imidazopyrimidine derivative **6a**.

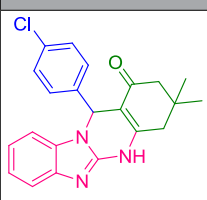
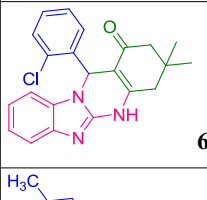
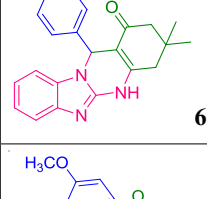
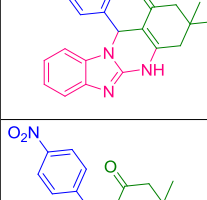
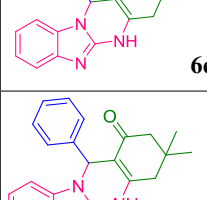
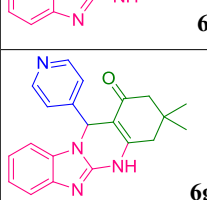
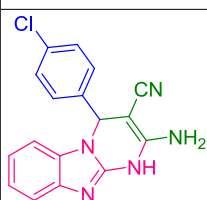
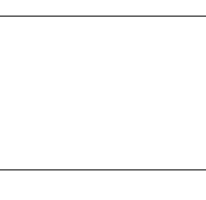


Reaction conditions: 2-aminobenzimidazole (**2**, 1 mmol) and 4-chlorobenzaldehyde (**3a**, 1 mmol) and dimedone (**4**, 1 mmol) under solvent-free conditions (unless solvent indicated, 2 mL). ^aIsolated yields.

delight, the use of Iron oxide@PMO-ICS-PrSO₃H (**1**) at 7 mg loading enhanced significantly the yield of the desired product **6a** under the same conditions (Table 1, entry 2). Increasing of the catalyst loading to 10 mg (Iron oxide@PMO-ICS-PrSO₃H, **1**) afforded higher yield of the desired product in shorter reaction time (entry 3). However, higher loading of the solid acid catalyst **1** had no significant impact on the yield and reaction time (entries 4,5). On the other hand, lower yields of the desired product **6a** were obtained when the model reaction was investigated at lower temperatures under same catalyst loading or solvent-free conditions at 80 °C (Table 1, entries 6–7). Furthermore, 12-(4-chlorophenyl)-3,3-dimethyl-1,2,3,4,5,12-hexahydrobenzo[4,5]imidazo[2,1-*b*]quinazolin-1-one (**6a**) was obtained in lower yields when the model reaction was investigated using 10 mg loading of Iron oxide@PMO-ICS-PrSO₃H (**1**) in other solvents such as EtOH/H₂O or THF under reflux conditions (Table 1, entries 8–9). Moreover, lower yields of the desired product **6a** was obtained in the presence of Iron oxide@PMO-ICS, Iron oxide@PMO-ICS-PrSH, iron oxide, or pure PMO-ICS under similar reaction conditions (10 mg catalyst loading, solvent-free conditions, 80 °C, Table 1, entries 10–13). These findings indicate that the catalytic activity of Iron oxide@PMO-ICS-PrSO₃H is mainly related to the existence of significant synergic effect of sulfonic acid groups (–SO₃H) along with iron oxide in this mesoporous catalyst. Furthermore, the Sheldon test was performed to show the heterogeneous nature of the magnetic catalyst **1** and verify possible leaching of the propylsulfonic acid groups to the reaction mixture¹⁰². Thus, the catalyst **1** was isolated from the reaction mixture by an external magnet after 5 min heating at 80 °C (10 mg catalyst loading) and the remaining mixture was heated for further 10 min. Indeed, only 57% of the desired product **6a** was isolated.

In the next step, the activity of the Iron oxide@PMO-ICS-PrSO₃H catalyst **1** in the synthesis of imidazopyrimidines derivatives was further investigated to other aromatic aldehydes **3b–h** or malononitrile C–H acid **5** using optimized conditions (10 mg Iron oxide@PMO-ICS-PrSO₃H loading under solvent-free conditions at 80 °C). Indeed, different derivatives of imidazopyrimidine were prepared in high to excellent yields via the condensation of 2-aminobenzimidazole (**2**), aromatic aldehydes **3a–g**, dimedone (**4**) or malononitrile (**5**) under optimal reaction conditions. As data in Table 2 show, various aromatic carbocyclic or heterocyclic aldehydes including both electron-withdrawing and electron-donating group were involved in the optimal reaction conditions to afford the desired products **6–7** in high to excellent yields (Table 2). In all studied cases, the reaction proceeded smoothly and the desired products were obtained without remaining any intermediates after reaction times indicated in Table 2. The obtained products were identified by the comparison of their spectral data and melting points with those reported for the valid samples.

According to the obtained results, a plausible mechanism for the synthesis of imidazopyrimidine derivatives **6a–g** and **7a–g** catalyzed by the Iron oxide@PMO-ICS-PrSO₃H nanocatalyst (**1**) is outlined in Scheme 2. At the first step, aldehydes **3** can be activated by the Iron oxide@PMO-ICS-PrSO₃H magnetic solid acid mainly through -PrSO₃H groups to afford the Knoevenagel condensation product of aldehydes **3** and dimedone (**4**) or

Entry	Aldehyde 3	C–H acid 4–5	Product 6–7	Time (min)	Yield ^a (%)	M.P [Lit.]
1	4-Chlorobenzaldehyde (3a)	4	 6a	15	95	336–339 ⁸⁰
2	2-Chlorobenzaldehyde (3b)	4	 6b	18	92	352–355 ⁸⁰
3	4-Methylbenzaldehyde (3c)	4	 6c	18	92	325–328 ¹⁰³
4	4-Methoxybenzaldehyde (3d)	4	 6d	20	90	385–388 ¹⁰⁴
5	4-Nitrobenzaldehyde (3e)	4	 6e	15	95	374–378 ¹⁰⁵
6	Benzaldehyde (3f)	4	 6f	25	88	308–310 ¹⁰⁶
7	4-Pyridinbenzaldehyde (3g)	4	 6g	14	95	298–300 ⁹²
8	4-Chlorobenzaldehyde (3a)	5	 7a	10	96	234–237 ⁸⁰
Continued						

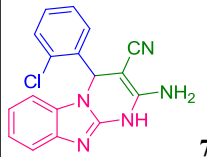
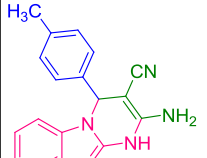
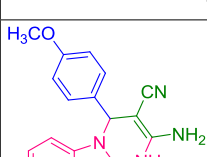
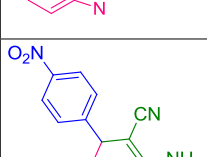
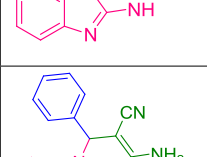
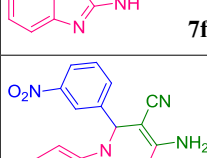
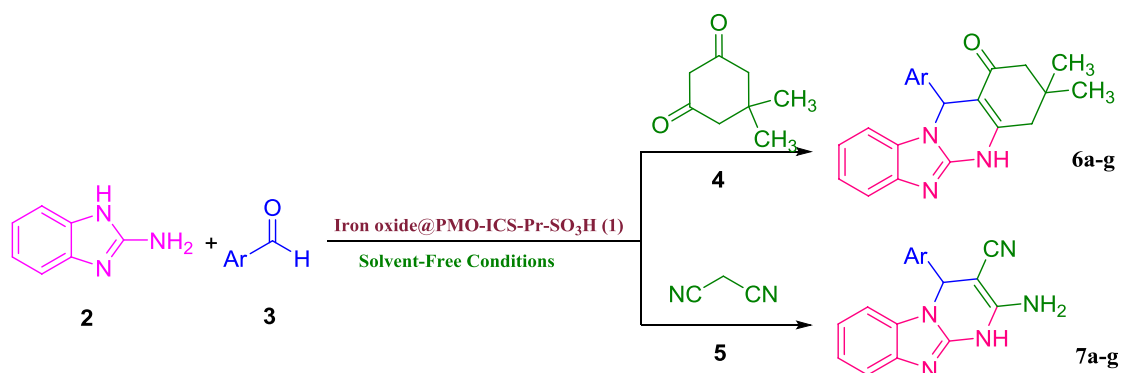
Entry	Aldehyde 3	C-H acid 4-5	Product 6-7	Time (min)	Yield ^a (%)	M.P [Lit.]
9	2-Chlorobenzaldehyde (3b)	5	 7b	15	93	236–238 ⁹²
10	4-Methylbenzaldehyde (3c)	5	 7c	14	92	189–201 ⁸⁰
11	4-Methoxybenzaldehyde (3d)	5	 7d	18	95	231–234 ⁸⁰
12	4-Nitrobenzaldehyde (3e)	5	 7e	12	94	345–348 ⁹²
13	Benzaldehyde (3f)	5	 7f	20	90	232–235 ¹⁰⁷
14	3-Nitrobenzaldehyde (3h)	5	 7g	18	93	235–237 ¹⁰⁷

Table 2. Synthesis of the imidazopyrimidine derivatives **6a–g** and **7a–g** in the presence of the Iron oxide@PMO-ICS-PrSO₃H nanocatalyt (**1**).



Reaction conditions: 2-aminobenzimidazole (**2**, 1 mmol) and 4-chlorobenzaldehyde (**3a**, 1 mmol) and dimedone (**4**, 1 mmol) in the presence of Iron oxide@PMO-ICS-PrSO₃H (**1**, 10 mg). ^aIsolated yields.

malononitrile (5) C–H acid as intermediates (II) or (II'), respectively. Then, condensation of these intermediates with 2-aminobenzimidazole (2) produces Michael acceptor intermediates (III) or (III'), respectively, in the presence of Iron oxide@PMO-ICS-PrSO₃H solid acid (1). Finally, the activated intermediates (III) or (III') by the mesoporous Iron oxide@PMO-ICS-PrSO₃H catalyst (1) involve in the intramolecular Michael addition and subsequent tautomerization to afford tetracyclic or tricyclic imidazopyrimidine derivatives 6a–g and 7a–g, respectively.

The recyclability of the Iron oxide@PMO-ICS-PrSO₃H catalyst (1) in the synthesis of imidazopyrimidine derivatives. In this part of our study, the recyclability of the Iron oxide@PMO-ICS-PrSO₃H catalyst (1) in the model reaction was investigated under optimized conditions. The catalyst was easily recovered from the reaction mixture by an external magnet in each run, then washed with water and EtOH and finally dried at 100 °C for 2 h before next run (Fig. 10). During the recycling experiments with the reactants of model reaction under the same reaction conditions, no significant change in the activity of the catalyst (1) was observed for at least five successive runs, which clearly demonstrates the stability of the catalyst in synthesis of imidazopyrimidine derivatives under optimized conditions.

Finally, to demonstrate the merits of the newly developed solid acid catalyst 1 in the synthesis of imidazopyrimidine derivatives, the present protocol has been compared with other methods and published reports. Table 3 summarizes these data.

Experimental section

General information. All chemicals and reagents were supplied by Aldrich or Merck chemical companies. Benzaldehyde was used as a fresh distilled sample and other aldehydes were used without further purification. Commercial Merck silica gel 60 coated with fluorescent indicator F254 on aluminium plates were used in thin layer chromatography (TLC) experiments to monitor the progress of reactions. Transmission electron microscope, TEM (Zeiss EM10C, Germany) was used to obtain TEM images. A MIRA3 instrument of TESCAN Company, Czech Republic was used to obtain field emission scanning electron microscopy (FESEM) images. XRD patterns were obtained using an X-ray powder X'Pert Pro PANalytical diffractometer with CuK α radiation source. Thermal gravimetric analysis (TGA) was accomplished by means of a Bahr company STA 504 instrument. An ASAP 2020 micromeritics equipment was used to determine the BET specific surface area of the catalyst. FTIR spectra were obtained using KBr disks on a Shimadzu FT IR-8400S spectrometer. Melting points were determined using a digital melting point Electrothermal 9,100 apparatus and are uncorrected. ¹H NMR (500 MHz) spectra were obtained using a Bruker DRX-500 AVANCE spectrometer in DMSO at ambient temperature. VSM analysis was performed using a Lakeshore 7,410 series instrument.

General procedure for the preparation of magnetic isocyanurate-based periodic mesoporous organosilica (Iron oxide@PMO-ICS) nanomaterials (B). Isocyanurate-based periodic mesoporous organosilica (PMO-ICS) nanomaterials (A) were prepared according to the procedure described in our previous publications^{34,98}. After that, PMO-ICS (A, 2.0 g) was dispersed in toluene (20 mL) and stirred for 20 min at room temperature. Then, FeCl₂·4H₂O (2.0 g) and FeCl₃·6H₂O (4.0 g) were added to the obtained mixture under nitrogen atmosphere. The reaction mixture was then heated in an oil bath at 80 °C for 1 h. Next, aqueous NH₃ (25% w/v, 20 mL) solution was added dropwise to the reaction mixture over 30 min and the reaction allowed to proceed further for 1 h at 80 °C. Then the obtained solid was washed with deionized H₂O/EtOH (50:50 v/v, 40 mL) and dried at 100 °C for 1 h.

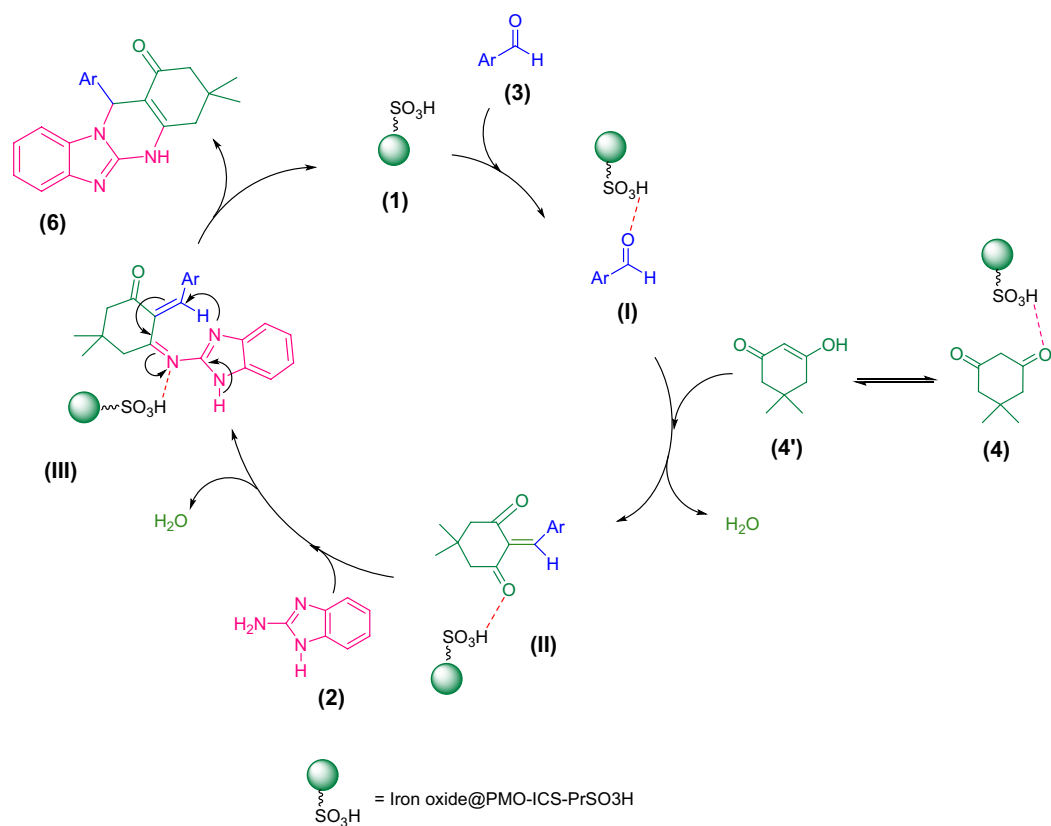
General procedure for the preparation of magnetic isocyanurate-based propylsulfonic acid periodic mesoporous organosilica (Iron oxide@PMO-ICS-PrSO₃H) nanomaterials (1). Iron oxide@PMO-ICS (B, 2.0 g) was dispersed in toluene (10 mL). Then, 0.4 mL of the 3-[(trimethoxysilyl) propyl] thiol was slowly added to the mixture and stirred at room temperature for 24 h to afford Iron oxide@PMO-ICS-PrSH (C). The resulting solid was filtered, washed by distilled water and dried under vacuum for 1 h. Finally, 1.0 g of Iron oxide@PMO-ICS-PrSH (C) was dispersed in deionized H₂O (4 mL) and H₂O₂ (6 mL) was slowly added to the above mixture stirred at room temperature for 24 h. The obtained black solid (Iron oxide@PMO-ICS-PrSO₃H, 1) was filtered off and washed with deionized water twice (15 mL) and then dried at 100 °C for 2 h.

General procedure for the synthesis of imidazopyrimidine derivatives 6/7 a-g catalyzed by Iron oxide@PMO-ICS-PrSO₃H nanomaterials (1). Iron oxide@PMO-ICS-PrSO₃H (1, 10 mg) was added to a mixture of 2-aminobenzimidazole (2, 1 mmol, 0.133 mg), aromatic aldehyde (3, 1 mmol), and dimedone or malononitrile (4-5, 1 mmol). The obtained reaction mixture was stirred under solvent-free conditions at 80 °C for the proper times indicated in Table 2. The progress of the reaction was monitored by TLC (EtOAc: n-hexane, 1:3). After completion of the reaction, DMF (2 mL) was added and the reaction mixture was heated to dissolve organic materials. The magnetic nanocatalyst 1 was then collected by an external magnet. After that, distilled water (5 mL) was added to the DMF solution and the obtained precipitate was filtered off and washed using n-hexane (2 mL) to afford pure products. The obtained powders were then dried in an oven at 80 °C for 1 h.

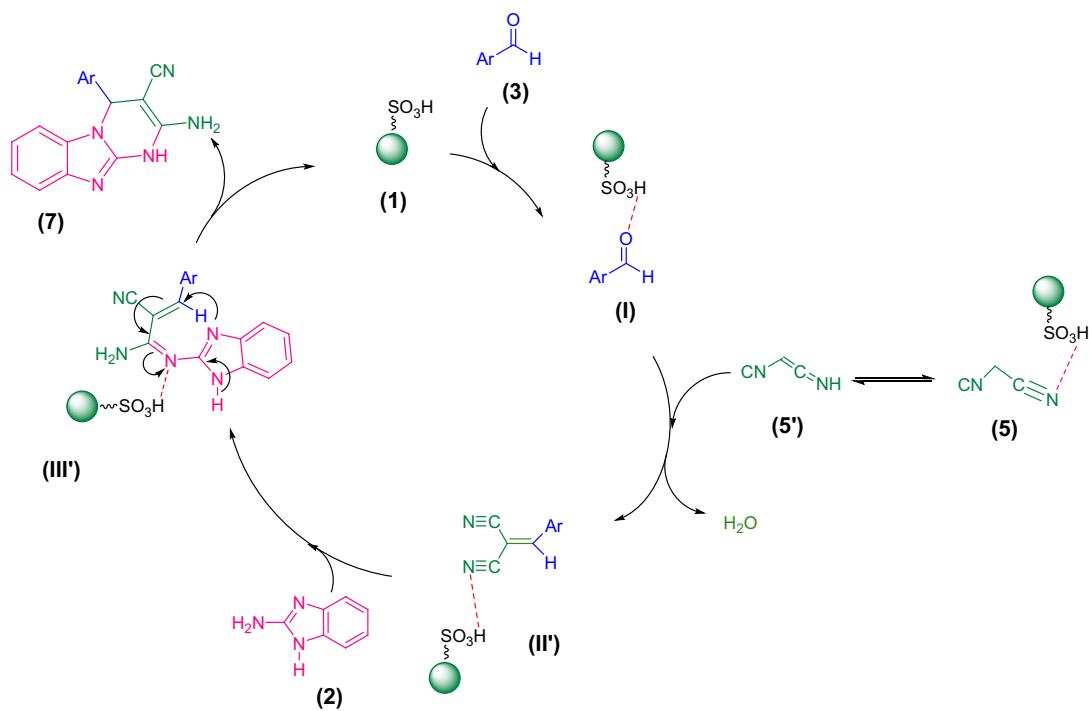
Conclusions

In summary, the novel and thermally stable magnetic isocyanurate-based propylsulfonic acid periodic mesoporous organosilica (Iron oxide@PMO-ICS-PrSO₃H) was prepared for the first time. The Iron oxide@PMO-ICS-PrSO₃H solid acid was used for highly efficient, facile, and green and sustainable synthesis of

Part A:



Part B:



Scheme 2. A plausible mechanism for the synthesis of imidazopyrimidine derivatives **6a–g** (Part A) and **7a–g** (Part B) in the presence of the Iron oxide@PMO-ICS-PrSO₃H nanocatalyst (**1**).



Figure 10. Investigation of the feasibility for reusing of Iron oxide@PMO-ICS-PrSO₃H magnetic mesoporous catalyst (1) in the synthesis of 12-(4-chlorophenyl)-3,3-dimethyl-1,2,3,4,5,12-hexahydrobenzo[4,5]imidazo[2,1-*b*]quinazolin-1-one (6a).

Entry	Catalyst	Catalyst loading	Solvent	Temp (°C)	Time (min)	Yield (%)	References
1	Fe ₃ O ₄ @GO	65 mg	EtOH	Reflux	125	94	²⁴
2	[PVP-SO ₃ H]HSO ₄	25 mg	Solvent-Free	90	14	96	⁴³
3	Fe ₃ O ₄ @IM	30 mg	EtOH	78	15	95	¹⁰
4	Nano-WO ₃ -SO ₃ H	19 mg	Solvent-Free	100	14	91	⁵
5	Fe ₃ O ₄ @SiO ₂ -ZrCl ₂ -MNP	25 mg	Solvent-Free	100	8	95	³²
6	Iron oxide@PMO-ICS-Pr-SO ₃ H	10 mg	Solvent-Free	80	10	95	This Work

Table 3. Comparison of the catalytic efficiency of the Iron oxide@PMO-ICS-PrSO₃H solid acid (1) with other catalytic systems for the synthesis of 6a.

12-phenyl-3,3-dimethyl-3,4,5,12-tetrahydrobenzo[4,5]imidazo[1,2-*b*]quinazolin-1(2*H*)-one or 2-amino-4-phenyl-1,4-dihydrobenzo[4,5]imidazo[1,2-*a*]pyrimidine-3-carbonitrile derivatives in a one-pot and three-component protocol through condensation of aldehydes, dimedone/malononitrile, and 2-aminobenzimidazole under solvent-free conditions. This methodology offers outstanding advantages including (i) high to excellent yields in shorter reaction times, (ii) low catalyst loading and cost and (iii) simple work-up procedure, fast separation of the catalyst, and catalyst recyclability.

Received: 5 March 2020; Accepted: 11 June 2020

Published online: 30 June 2020

References

- Climent, M. J., Corma, A. & Iborra, S. Heterogeneous catalysts for the one-pot synthesis of chemicals and fine chemicals. *Chem. Rev.* **111**, 1072–1133 (2011).
- Clark, J. H. In *Heterogeneous Catalysts for Clean Technology* (eds Wilson, K. & Lee, A. F.) Ch. 1, 1–10 (Wiley-VCH, 2013).
- Li, Z. *et al.* Well-defined materials for heterogeneous catalysis: from nanoparticles to isolated single-atom sites. *Chem. Rev.* **120**, 623–682. <https://doi.org/10.1021/acs.chemrev.9b00311> (2020).
- Bystrzanowska, M., Petkov, P. & Tobiszewski, M. Ranking of heterogeneous catalysts metals by their greenness. *ACS Sustain. Chem. Eng.* **7**, 18434–18443. <https://doi.org/10.1021/acssuschemeng.9b04230> (2019).
- Sheldon, R. A., Arends, I. & Hanefeld, U. *Green Chemistry and Catalysis* (Wiley, London, 2007).
- Astruc, D., Lu, F. & Aranzas, J. R. Nanoparticles as recyclable catalysts: the frontier between homogeneous and heterogeneous catalysis. *Angew. Chem. Int. Ed.* **44**, 7852–7872. <https://doi.org/10.1002/anie.200500766> (2005).
- Varma, R. S. Editorial overview: sustainability via nanocatalysis. *Curr. Opin. Green Sustain. Chem.* **15**, A1–A3. <https://doi.org/10.1016/j.cogsc.2018.12.002> (2019).
- Alzeer, M. I. & MacKenzie, K. J. Synthesis and catalytic properties of new sustainable aluminosilicate heterogeneous catalysts derived from fly ash. *ACS Sustain. Chem. Eng.* **6**, 5273–5282 (2018).
- Liu, L. & Corma, A. Metal catalysts for heterogeneous catalysis: from single atoms to nanoclusters and nanoparticles. *Chem. Rev.* **118**, 4981–5079. <https://doi.org/10.1021/acs.chemrev.7b00776> (2018).
- Cuenya, B. R. & Beharfarid, F. Nanocatalysis: size- and shape-dependent chemisorption and catalytic reactivity. *Surf. Sci. Rep.* **70**, 135–187 (2015).
- Hatton, B., Landskron, K., Whitnall, W., Perovic, D. & Ozin, G. A. Past, present, and future of periodic mesoporous organosilicas the PMOs. *Acc. Chem. Res.* **38**, 305–312. <https://doi.org/10.1021/ar040164a> (2005).
- Matsukawa, H. *et al.* Fast and stable vapochromic response induced through nanocrystal formation of a luminescent platinum(II) complex on periodic mesoporous organosilica. *Sci. Rep.* **9**, 15151. <https://doi.org/10.1038/s41598-019-51615-w> (2019).
- Wei, Y. *et al.* Periodic mesoporous organosilica nanocubes with ultrahigh surface areas for efficient CO₂ adsorption. *Sci. Rep.* **6**, 20769 (2016).

14. Chanson, R. *et al.* Damage-free plasma etching of porous organo-silicate low-k using micro-capillary condensation above—50° C. *Sci. Rep.* **8**, 1–12 (2018).
15. Matsukawa, H. *et al.* Fast and stable vapochromic response induced through nanocrystal formation of a luminescent platinum (II) complex on periodic mesoporous organosilica. *Sci. Rep.* **9**, 1–11 (2019).
16. Olkhoviyk, O. & Jaroniec, M. In *Environmental Applications of Nanomaterials: Synthesis, Sorbents and Sensors* 179–212 (Imperial College Press London, 2007).
17. Park, S. S., Moorthy, M. S. & Ha, C.-S. Periodic mesoporous organosilicas for advanced applications. *NPG Asia Mater.* **6**, e96–e96 (2014).
18. Waki, M. & Inagaki, S. Periodic mesoporous organosilicas possessing molecularly mixed pyridine and benzene moieties in the frameworks. *Microporous Mesoporous Mater.* **284**, 10–15. <https://doi.org/10.1016/j.micromeso.2019.04.007> (2019).
19. Valimaña-Traverso, J. *et al.* Periodic mesoporous organosilica materials as sorbents for solid-phase extraction of drugs prior to simultaneous enantiomeric separation by capillary electrophoresis. *J. Chromatogr. A* **1566**, 135–145. <https://doi.org/10.1016/j.chroma.2018.06.043> (2018).
20. Ishikawa, S., Maegawa, Y., Waki, M. & Inagaki, S. Well-controlled radical-based epoxidation catalyzed by copper complex immobilized on bipyridine-periodic mesoporous organosilica. *Appl. Catal. A* **575**, 87–92. <https://doi.org/10.1016/j.apcata.2019.02.007> (2019).
21. Ryzhikov, A. *et al.* Periodic mesoporous organosilicas as porous matrix for heterogeneous lyophobic systems. *Microporous Mesoporous Mater.* **260**, 166–171. <https://doi.org/10.1016/j.micromeso.2017.10.037> (2018).
22. Wu, L. *et al.* Sulfonated periodic-mesoporous-organosilicas column for selective separation of C₂H₂/CH₄ mixtures. *J. Solid State Chem.* **264**, 113–118. <https://doi.org/10.1016/j.jssc.2018.03.038> (2018).
23. Teng, Z. *et al.* A facile multi-interface transformation approach to monodisperse multiple-shelled periodic mesoporous organosilica hollow spheres. *J. Am. Chem. Soc.* **137**, 7935–7944. <https://doi.org/10.1021/jacs.5b05369> (2015).
24. Yoshida, M. *et al.* Immobilization of luminescent Platinum(II) complexes on periodic mesoporous organosilica and their water reduction photocatalysis. *J. Photochem. Photobiol. A* **358**, 334–344. <https://doi.org/10.1016/j.jphotochem.2017.09.008> (2018).
25. Rebbin, V., Schmidt, R. & Fröba, M. Spherical particles of phenylene-bridged periodic mesoporous organosilica for high-performance liquid chromatography. *Angew. Chem. Int. Ed.* **45**, 5210–5214. <https://doi.org/10.1002/anie.200504568> (2006).
26. Granadeiro, C. M. *et al.* A novel red emitting material based on polyoxometalate@periodic mesoporous organosilica. *Microporous Mesoporous Mater.* **234**, 248–256. <https://doi.org/10.1016/j.micromeso.2016.07.023> (2016).
27. Ma, X. *et al.* Hollow periodic mesoporous organosilica nanospheres by a facile emulsion approach. *J. Colloid Interface Sci.* **475**, 66–71. <https://doi.org/10.1016/j.jcis.2016.04.026> (2016).
28. Cornelius, M., Hoffmann, F. & Fröba, M. Periodic mesoporous organosilicas with a bifunctional conjugated organic unit and crystal-like pore walls. *Chem. Mater.* **17**, 6674–6678. <https://doi.org/10.1021/cm051935n> (2005).
29. Wang, W., Grozea, D., Kohli, S., Perovic, D. D. & Ozin, G. A. Water repellent periodic mesoporous organosilicas. *ACS Nano* **5**, 1267–1275. <https://doi.org/10.1021/nn102929t> (2011).
30. Ha, C.-S. & Park, S. S. In *Periodic Mesoporous Organosilicas* 125–187 (Springer, 2019).
31. Karimi, B., Rostami, F. B., Khorasani, M., Elhamifar, D. & Vali, H. Selective oxidation of alcohols with hydrogen peroxide catalyzed by tungstate ions (WO₄⁼) supported on periodic mesoporous organosilica with imidazolium frameworks (PMO-IL). *Tetrahedron* **70**, 6114–6119. <https://doi.org/10.1016/j.tet.2014.04.030> (2014).
32. Norouzi, M. & Elhamifar, D. Phenylene and isatin based bifunctional mesoporous organosilica supported schiff-base/manganese complex: an efficient and recoverable nanocatalyst. *Catal. Lett.* **149**, 619–628 (2019).
33. Elhamifar, D. & Ardeshtifard, H. Phenyl and ionic liquid based bifunctional periodic mesoporous organosilica supported copper: an efficient nanocatalyst for clean production of polyhydroquinolines. *J. Colloid Interface Sci.* **505**, 1177–1184 (2017).
34. Yaghoubi, A., Dekamin, M. G., Arefi, E. & Karimi, B. Propylsulfonic acid-anchored isocyanurate-based periodic mesoporous organosilica (PMO-ICS-Pr-SO₃H): a new and highly efficient recoverable nanoporous catalyst for the one-pot synthesis of bis(indolyl) methane derivatives. *J. Colloid Interface Sci.* **505**, 956–963 (2017).
35. Dekamin, M. G., Arefi, E. & Yaghoubi, A. Isocyanurate-based periodic mesoporous organosilica (PMO-ICS): a highly efficient and recoverable nanocatalyst for the one-pot synthesis of substituted imidazoles and benzimidazoles. *RSC Adv.* **6**, 86982–86988 (2016).
36. Manayil, J. C., Lee, A. F. & Wilson, K. Functionalized periodic mesoporous organosilicas: tunable hydrophobic solid acids for biomass conversion. *Molecules* **24**, 239 (2019).
37. De Canck, E., Dosuna-Rodríguez, I., Gaigneaux, E. M. & Van Der Voort, P. Periodic mesoporous organosilica functionalized with sulfonic acid groups as acid catalyst for glycerol acetylation. *Materials* **6**, 3556–3570 (2013).
38. Corma, A., Das, D., García, H. & Leyva, A. A periodic mesoporous organosilica containing a carbapalladacycle complex as heterogeneous catalyst for Suzuki cross-coupling. *J. Catal.* **229**, 322–331. <https://doi.org/10.1016/j.jcat.2004.11.006> (2005).
39. Borah, P., Ma, X., Nguyen, K. T. & Zhao, Y. A vanadyl complex grafted to periodic mesoporous organosilica: a green catalyst for selective hydroxylation of benzene to phenol. *Angew. Chem. Int. Ed.* **51**, 7756–7761. <https://doi.org/10.1002/anie.201203275> (2012).
40. Karimi, B. & Esfahani, F. K. Unexpected golden Ullmann reaction catalyzed by Au nanoparticles supported on periodic mesoporous organosilica (PMO). *Chem. Commun.* **47**, 10452–10454 (2011).
41. Kaczmarek, A. M. *et al.* Amine-containing (nano-) periodic mesoporous organosilica and its application in catalysis, sorption and luminescence. *Microporous Mesoporous Mater.* **291**, 109687. <https://doi.org/10.1016/j.micromeso.2019.109687> (2020).
42. Olkhoviyk, O. & Jaroniec, M. Periodic mesoporous organosilica with large heterocyclic bridging groups. *J. Am. Chem. Soc.* **127**, 60–61. <https://doi.org/10.1021/ja043941a> (2005).
43. Cho, E.-B., Kim, D. & Jaroniec, M. Bifunctional periodic mesoporous organosilicas with thiophene and isocyanurate bridging groups. *Langmuir* **25**, 13258–13263. <https://doi.org/10.1021/la902089c> (2009).
44. Yaghoubi, A., Dekamin, M. G. & Karimi, B. Propylsulfonic acid-anchored isocyanurate-based periodic mesoporous organosilica (PMO-ICS-PrSO₃H): a highly efficient and recoverable nanoporous catalyst for the one-pot synthesis of substituted polyhydroquinolines. *Catal. Lett.* **147**, 2656–2663. <https://doi.org/10.1007/s10562-017-2159-5> (2017).
45. Dekamin, M. G., Varmira, K., Farahmand, M., Sagheb-Asl, S. & Karimi, Z. Organocatalytic, rapid and facile cyclotrimerization of isocyanates using tetrabutylammonium phthalimide-N-oxyl and tetraethylammonium 2-(carbamoyl)benzoate under solvent-free conditions. *Catal. Commun.* **12**, 226–230. <https://doi.org/10.1016/j.catcom.2010.08.018> (2010).
46. Dekamin, M. G., Moghaddam, F. M., Saeidian, H. & Mallakpour, S. The performance of phthalimide-N-oxyl anion. *Monatsh für Chemie / Chem. Monthly* **137**, 1591–1595. <https://doi.org/10.1007/s00706-006-0553-6> (2006).
47. Moghaddam, F. M., Dekamin, M. G., Khajavi, M. S. & Jalili, S. Efficient and selective trimerization of aryl and alkyl isocyanates catalyzed by sodium p-toluenesulfonate in the presence of TBAI in a solvent-free condition. *Bull. Chem. Soc. Jpn.* **75**, 851–852. <https://doi.org/10.1246/bcsj.75.851> (2002).
48. Arsalani, S., Guidelli, E. J., Araujo, J. F., Bruno, A. C. & Baffa, O. Green synthesis and surface modification of iron oxide nanoparticles with enhanced magnetization using natural rubber latex. *ACS Sustain. Chem. Eng.* **6**, 13756–13765 (2018).
49. Nguyen, M. T. *et al.* Green synthesis of size-tunable iron oxides and iron nanoparticles in a salt matrix. *ACS Sustain. Chem. Eng.* **7**, 17697–17705. <https://doi.org/10.1021/acssuschemeng.9b03950> (2019).

50. Xun, S. *et al.* Magnetic mesoporous nanospheres supported phosphomolybdate-based ionic liquid for aerobic oxidative desulfurization of fuel. *J. Colloid Interface Sci.* **534**, 239–247. <https://doi.org/10.1016/j.jcis.2018.08.115> (2019).
51. Ishani, M., Dekamin, M. G. & Alirezvani, Z. Superparamagnetic silica core-shell hybrid attached to graphene oxide as a promising recoverable catalyst for expeditious synthesis of TMS-protected cyanohydrins. *J. Colloid Interface Sci.* **521**, 232–241. <https://doi.org/10.1016/j.jcis.2018.02.060> (2018).
52. Alirezvani, Z., Dekamin, M. G. & Valiey, E. Cu(II) and magnetite nanoparticles decorated melamine-functionalized chitosan: a synergistic multifunctional catalyst for sustainable cascade oxidation of benzyl alcohols/Knoevenagel condensation. *Sci. Rep.* **9**, 17758. <https://doi.org/10.1038/s41598-019-53765-3> (2019).
53. Doustkhah, E. *et al.* Merging periodic mesoporous organosilica (PMO) with mesoporous aluminosilica (Al/Si-PMO): a catalyst for green oxidation. *Mol. Catal.* **482**, 110676 (2020).
54. Dai, J. *et al.* Yolk-shell Fe₃O₄@SiO₂@PMO: amphiphilic magnetic nanocomposites as an adsorbent and a catalyst with high efficiency and recyclability. *Green Chem.* **19**, 1336–1344. <https://doi.org/10.1039/C6GC02926D> (2017).
55. Haghghat, M., Shirini, F. & Golshekan, M. Efficiency of NaHSO₄ modified periodic mesoporous organosilica magnetic nanoparticles as a new magnetically separable nanocatalyst in the synthesis of [1,2,4]triazoloquinazolinone/pyrimidine derivatives. *J. Mol. Struct.* **1171**, 168–178. <https://doi.org/10.1016/j.molstruc.2018.05.112> (2018).
56. Haghghat, M., Shirini, F. & Golshekan, M. Synthesis of tetrahydrobenzo[b]pyran and pyrano[2, 3-d]pyrimidinone derivatives using Fe₃O₄@Ph-PMO-NaHSO₄ as a new magnetically separable nanocatalyst. *J. Nanosci. Nanotechnol.* **19**, 3447–3458. <https://doi.org/10.1166/jnn.2019.16032> (2019).
57. Boukis, A. C., Reiter, K., Frölich, M., Hofheinz, D. & Meier, M. A. R. Multicomponent reactions provide key molecules for secret communication. *Nat. Commun.* **9**, 1439. <https://doi.org/10.1038/s41467-018-03784-x> (2018).
58. Ugi, I., Domling, A. & Werner, B. Since 1995 the new chemistry of multicomponent reactions and their libraries, including their heterocyclic chemistry. *J. Heterocycl. Chem.* **37**, 647–658. <https://doi.org/10.1002/jhet.5570370322> (2000).
59. Xiong, Q., Dong, S., Chen, Y., Liu, X. & Feng, X. Asymmetric synthesis of tetrazole and dihydroisoquinoline derivatives by isocyanide-based multicomponent reactions. *Nat. Commun.* **10**, 2116. <https://doi.org/10.1038/s41467-019-09904-5> (2019).
60. Isambert, N. *et al.* Multicomponent reactions and ionic liquids: a perfect synergy for eco-compatible heterocyclic synthesis. *Chem. Soc. Rev.* **40**, 1347–1357. <https://doi.org/10.1039/C0CS00013B> (2011).
61. Balou, J., Khalilzadeh, M. A. & Zareyee, D. An efficient and reusable nano catalyst for the synthesis of benzoxanthene and chromene derivatives. *Sci. Rep.* **9**, 3605. <https://doi.org/10.1038/s41598-019-40431-x> (2019).
62. Zhang, J. *et al.* Exploring ugi-azide four-component reaction products for broad-spectrum influenza antivirals with a high genetic barrier to drug resistance. *Sci. Rep.* **8**, 4653. <https://doi.org/10.1038/s41598-018-22875-9> (2018).
63. Rudick, J. G., Shaabani, S. & Dömling, A. Editorial: isocyanide-based multicomponent reactions. *Front. Chem.* <https://doi.org/10.3389/fchem.2019.00918> (2020).
64. Konrad, W. *et al.* A combined photochemical and multicomponent reaction approach to precision oligomers. *Chem. A Eur. J.* **24**, 3413–3419. <https://doi.org/10.1002/chem.201705939> (2018).
65. Kakuchi, R. The dawn of polymer chemistry based on multicomponent reactions. *Polym. J.* **51**, 945–953. <https://doi.org/10.1038/s41428-019-0209-0> (2019).
66. Meier, M. A. R. & Barner-Kowollik, C. A new class of materials: sequence-defined macromolecules and their emerging applications. *Adv. Mater.* **31**, 1806027. <https://doi.org/10.1002/adma.201806027> (2019).
67. Afshari, R. & Shaabani, A. Materials functionalization with multicomponent reactions: state of the art. *ACS Comb. Sci.* **20**, 499–528. <https://doi.org/10.1021/acscmbosci.8b00072> (2018).
68. Zhou, H., Su, G., Jiao, P. & Yan, B. Accelerating the multifunctionalization of therapeutic nanoparticles by using a multicomponent reaction. *Chem. A Eur. J.* **18**, 5501–5505. <https://doi.org/10.1002/chem.201103743> (2012).
69. Ruijter, E., Scheffelaar, R. & Orri, R. V. Multicomponent reaction design in the quest for molecular complexity and diversity. *Angew. Chem. Int. Ed.* **50**, 6234–6246 (2011).
70. Ganem, B. Strategies for innovation in multicomponent reaction design. *Acc. Chem. Res.* **42**, 463–472. <https://doi.org/10.1021/ar800214s> (2009).
71. Alvim, H. G., da Silva Junior, E. N. & Neto, B. A. What do we know about multicomponent reactions? Mechanisms and trends for the Biginelli, Hantzsch, Mannich, Passerini and Ugi MCRs. *Rsc Adv.* **4**, 54282–54299 (2014).
72. Zolfigol, M. A., Yarie, M. & Bagheri, S. [4, 4'-Bipyridine]-1, 1'-dium tricyanomethanide as a nanostructured molten salt and its catalytic application in the synthesis of tetrahydrobenzo [b] pyrans, amido and aminoalkyl naphthol derivatives. *J. Mol. Liq.* **222**, 923–932 (2016).
73. Dekamin, M. G., Eslami, M. & Maleki, A. Potassium phthalimide-N-oxyl: a novel, efficient, and simple organocatalyst for the one-pot three-component synthesis of various 2-amino-4H-chromene derivatives in water. *Tetrahedron* **69**, 1074–1085 (2013).
74. Dekamin, M. G., Azimoshan, M. & Ramezani, L. Chitosan: a highly efficient renewable and recoverable bio-polymer catalyst for the expeditious synthesis of α -amino nitriles and imines under mild conditions. *Green Chem.* **15**, 811–820 (2013).
75. Eckert, H. Diversity oriented syntheses of conventional heterocycles by smart multi component reactions (MCRs) of the last decade. *Molecules (Basel, Switzerland)* **17**, 1074–1102. <https://doi.org/10.3390/molecules17011074> (2012).
76. Yu, J., Shi, F. & Gong, L.-Z. Brønsted-acid-catalyzed asymmetric multicomponent reactions for the facile synthesis of highly enantioenriched structurally diverse nitrogenous heterocycles. *Acc. Chem. Res.* **44**, 1156–1171. <https://doi.org/10.1021/ar2000343> (2011).
77. Bagdi, A. K., Santra, S., Monir, K. & Hajra, A. Synthesis of imidazo[1,2-a]pyridines: a decade update. *Chem. Commun.* **51**, 1555–1575. <https://doi.org/10.1039/C4CC08495K> (2015).
78. Goodacre, S. C. *et al.* Imidazo [1, 2-a] pyrimidines as functionally selective and orally bioavailable GABAA α 2/ α 3 binding site agonists for the treatment of anxiety disorders. *J. Med. Chem.* **49**, 35–38 (2006).
79. Kaur, N. *et al.* One-pot synthesis of tricyclic dihydropyrimidine derivatives and their biological evaluation. *Tetrahedron* **71**, 332–337. <https://doi.org/10.1016/j.tet.2014.11.039> (2015).
80. Hemmati, B., Javanshir, S. & Dolatkah, Z. Hybrid magnetic Irish moss/Fe₃O₄ as a nano-biocatalyst for synthesis of imidazo-pyrimidine derivatives. *RSC Adv.* **6**, 50431–50436 (2016).
81. Protopopov, M. V. *et al.* Dihydrobenzo[4,5]imidazo[1,2-a]pyrimidine-4-ones as a new class of CK2 inhibitors. *Mol. Diversity* **22**, 991–998. <https://doi.org/10.1007/s11030-018-9836-1> (2018).
82. Ebajo, V. D., Santos, C. R. L., Alea, G. V., Lin, Y. A. & Chen, C.-H. Regenerable acidity of graphene oxide in promoting multicomponent organic synthesis. *Sci. Rep.* **9**, 15579. <https://doi.org/10.1038/s41598-019-51833-2> (2019).
83. Heravi, M. M. *et al.* A three component one-pot procedure for the synthesis of [1, 2, 4] triazolo/benzimidazolo-quinazolinone derivatives in the presence of H₆P₂W₁₈O₆₂·18H₂O as a green and reusable catalyst. *Mol. Diversity* **12**, 181–185 (2008).
84. Amoozadeh, A. & Rahmani, S. Nano-WO₃-supported sulfonic acid: New, efficient and high reusable heterogeneous nano catalyst. *J. Mol. Catal. A: Chem.* **396**, 96–107 (2015).
85. Goli-Jolodar, O., Shirini, F. & Seddighi, M. Introduction of O-sulfonated poly (vinylpyrrolidonium) hydrogen sulfate as an efficient, and reusable solid acid catalyst for some solvent-free multicomponent reactions. *RSC Adv.* **6**, 44794–44806 (2016).
86. Raj, T. *et al.* “Solvent-less” mechanochemical approach to the synthesis of pyrimidine derivatives. *ACS Sustain. Chem. Eng.* **5**, 1468–1475. <https://doi.org/10.1021/acssuschemeng.6b02030> (2017).

87. Hamidinasab, M. & Mobinikhaledi, A. Organoacid-decorated NiFe₂O₄ nanoparticles: an efficient catalyst for green synthesis of 2H-indazolo[2, 1-b]phthalazine-triones and pyrimido[1,2-a]benzimidazoles. *Chem.Sel.* **4**, 17–23. <https://doi.org/10.1002/slct.201802413> (2019).
88. Maleki, A. & Rahimi, J. Synthesis of dihydroquinazolinone and octahydroquinazolinone and benzimidazoloquinazolinone derivatives catalyzed by an efficient magnetically recoverable GO-based nanocomposite. *J. Porous Mater.* **25**, 1789–1796 (2018).
89. Karimi, M. & Naimi-Jamal, M. Carboxymethyl cellulose as a green and biodegradable catalyst for the solvent-free synthesis of benzimidazoloquinazolinone derivatives. *J. Saudi Chem. Soc.* **23**, 182–187 (2019).
90. Heravi, M. M., Derikvand, F. & Ranjbar, L. Sulfamic acid-catalyzed, three-component, one-pot synthesis of [1, 2, 4] triazolo/benzimidazolo quinazolinone derivatives. *Synth. Commun.* **40**, 677–685 (2010).
91. Reddy, M. V., Oh, J. & Jeong, Y. T. p-Toluenesulfonic acid-catalyzed one-pot synthesis of 2-amino-4-substituted-1,4-dihydrobenzo[4,5]imidazo[1,2-a]pyrimidine-3-carbonitriles under neat conditions. *C. R. Chim.* **17**, 484–489. <https://doi.org/10.1016/j.crci.2013.08.007> (2014).
92. Mousavi, M. R. & Maghsoodlou, M. T. Catalytic systems containing p-toluenesulfonic acid monohydrate catalyzed the synthesis of triazoloquinazolinone and benzimidazoquinazolinone derivatives. *Monatshefte für Chemie-Chem. Mon.* **145**, 1967–1973 (2014).
93. Maleki, A. & Aghaei, M. Ultrasonic assisted synergetic green synthesis of polycyclic imidazo (thiazolo) pyrimidines by using Fe₃O₄@ clay core-shell. *Ultrason. Sonochem.* **38**, 585–589 (2017).
94. Kalita, S. J., Deka, D. C. & Mecadon, H. Organocatalytic domino Knöevenagel-Michael reaction in water for the regioselective synthesis of benzo [4, 5] imidazo [1, 2-a] pyrimidines and pyrido [2, 3-d] pyrimidin-2-amines. *RSC Adv.* **6**, 91320–91324 (2016).
95. Puligoundla, R. G. *et al.* A simple, convenient one-pot synthesis of [1,2,4]triazolo/benzimidazolo quinazolinone derivatives by using molecular iodine. *Tetrahedron Lett.* **54**, 2480–2483. <https://doi.org/10.1016/j.tetlet.2013.02.099> (2013).
96. Reddy, M. V., Byeon, K. R., Park, S. H. & Kim, D. W. Polyethylene glycol methacrylate-grafted dicationic imidazolium-based ionic liquid: heterogeneous catalyst for the synthesis of aryl-benzo [4, 5] imidazo [1, 2-a] pyrimidine amines under solvent-free conditions. *Tetrahedron* **73**, 5289–5296 (2017).
97. Dekamin, M. G., Karimi, Z. & Farahmand, M. Tetraethylammonium 2-(N-hydroxycarbamoyl) benzoate: a powerful bifunctional metal-free catalyst for efficient and rapid cyanosilylation of carbonyl compounds under mild conditions. *Catal. Sci. Technol.* **2**, 1375–1381 (2012).
98. Yaghoubi, A. & Dekamin, M. G. Green and facile synthesis of 4H-pyran scaffold catalyzed by pure nano-ordered periodic mesoporous organosilica with isocyanurate framework (PMO-ICS). *ChemistrySelect* **2**, 9236–9243 (2017).
99. Alirezvani, Z., Dekamin, M. G. & Valiey, E. New hydrogen-bond-enriched 1,3,5-tris(2-hydroxyethyl) isocyanurate covalently functionalized MCM-41: an efficient and recoverable hybrid catalyst for convenient synthesis of acridinedione derivatives. *ACS Omega* **4**, 20618–20633. <https://doi.org/10.1021/acsomega.9b02755> (2019).
100. Goodwill, P. W. *et al.* X-Space MPI: magnetic nanoparticles for safe medical imaging. *Adv. Mater.* **24**, 3870–3877. <https://doi.org/10.1002/adma.201200221> (2012).
101. Ghazanfari, M. R., Kashfi, M., Shams, S. F. & Jaafari, M. R. Perspective of Fe₃O₄ nanoparticles role in biomedical applications. *Biochem. Res. Int.* **2016**, 32. <https://doi.org/10.1155/2016/7840161> (2016).
102. Sheldon, R. A., Arends, I. W. C. E. & Hanefeld, U. In *Green Chemistry and Catalysis* Ch. 1, 1–47 (Wily-VCH, 2007).
103. Yao, C. *et al.* Three-component synthesis of 4-aryl-1H-pyrimido [1, 2-a] benzimidazole derivatives in ionic liquid. *J. Heterocycl. Chem.* **47**, 26–32 (2010).
104. Lipson, V. *et al.* Cyclocondensation of 2-aminobenzimidazole with dimedone and its arylidene derivatives. *Chem. Heterocycl. Compd.* **39**, 1041–1047 (2003).
105. Mousavi, M. R. & Maghsoodlou, M. T. Nano-SiO₂: a green, efficient, and reusable heterogeneous catalyst for the synthesis of quinazolinone derivatives. *J. Iran. Chem. Soc.* **12**, 743–749 (2015).
106. Weber, L. Multi-component reactions and evolutionary chemistry. *Drug Discovery Today* **7**, 143–147 (2002).
107. Shaabani, A. *et al.* Clean synthesis in water: uncatalyzed three-component condensation reaction of 3-amino-1,2,4-triazole or 2-aminobenzimidazole with aldehyde in the presence of activated CH-acids. *QSAR Comb. Sci.* **26**, 973–979. <https://doi.org/10.1002/qsar.200620024> (2007).

Acknowledgements

We are grateful for the financial support from The Research Council of Iran University of Science and Technology (IUST), Tehran, Iran (Grant No 160/19108). We would also like to acknowledge the support of The Iran Nanotechnology Initiative Council (INIC).

Author contributions

(1) Arezoo Akbari worked on the topic as her MSc. Thesis and prepared the initial draft of the manuscript. (2) Prof. Mohammad G. Dekamin is the first supervisor of Miss Akbari and Dr. Amene Yaghoubi as his MSc. and Ph.D. students, respectively. Also, he edited and revised the manuscript completely. (3) Dr. Amene Yaghoubi worked closely with Miss Akbari for doing experimental section and interpreting of the characterization data. (4) Prof. Mohammad Reza Naimi-Jamal is the second supervisor of Miss Akbari and edited initial draft of the manuscript.

Competing interests

The authors declare no competing interests.

Additional information

Correspondence and requests for materials should be addressed to M.G.D.

Reprints and permissions information is available at www.nature.com/reprints.

Publisher's note Springer Nature remains neutral with regard to jurisdictional claims in published maps and institutional affiliations.



Open Access This article is licensed under a Creative Commons Attribution 4.0 International License, which permits use, sharing, adaptation, distribution and reproduction in any medium or format, as long as you give appropriate credit to the original author(s) and the source, provide a link to the Creative Commons license, and indicate if changes were made. The images or other third party material in this article are included in the article's Creative Commons license, unless indicated otherwise in a credit line to the material. If material is not included in the article's Creative Commons license and your intended use is not permitted by statutory regulation or exceeds the permitted use, you will need to obtain permission directly from the copyright holder. To view a copy of this license, visit <http://creativecommons.org/licenses/by/4.0/>.

© The Author(s) 2020